THE PUBLISHING HOUSE
OF THE ROMANIAN ACADEMY

PROCEEDINGS OF THE ROMANIAN ACADEMY, Series A,
Volume 24, Number 2/2023, pp. 129–134
DOI: 10.59277/PRA-SER.A.24.2.04

SURFACE DIELECTRIC BARRIER DISCHARGE ON LOCALLY BULGED MATERIAL

Yichao YUAN, Mingliang SU, Shen ZHAO, Wei ZHANG, Chuliang DONG

Shanxi University, School of Power, Civil Engineering and Architecture
Corresponding author: Yichao YUAN, E-mail: 202023504039@email.sxu.edu.cn

Abstract. The propagation of atmospheric pressure streamer on the locally bulged dielectric material is essential for plasma catalysis and functionalizing biomedical materials. Such functionalization improves the uniformity of the treatment on the barrier surface. The characteristics of the streamer propagating depend on the bulged surface conditions. In this work, a two-dimensional self-consistent fluid model was built to study surface dielectric barrier discharge (SDBD) with bulges on the surface of the dielectric barrier, including electron density distribution, surface charge density evolution, and other electric parameters. It is demonstrated that with the increase of bulges' height, the streamer strides over the gaps between the bulges. Two branches of surface charge move along the surface of bulge from the left side of it. The existence of bulges with smaller curvature extend the propagation length of the streamer.

Key words*:* surface dielectric barrier discharge, streamer propagation, locally bulged material.

1. INTRODUCTION

In the last few decades, low-temperature plasma has been widely investigated and used in many applications. The main idea is to find out how the charged species, reactive neutral particles and electric field can improve the efficiency on surface treatment and biomedical applications [1, 2]. Corona discharge and dielectric barrier discharge have been used as plasma sources to functionalized polymers, improving adhesion, and the hydrophilic nature of the dielectric surface [3-5]. However, previous researches are mainly focused on the flat barrier surface, actually, it is not idealized flat of the dielectric barrier surface. The bulges will significantly change the performance of barrier materials in the traditional applications. By designing the arrangement of metal micro-structure units, electromagnetic meta-materials can show negative permittivity, negative permeability and negative refraction [6], with pattern composited of local bulges and voids. What's more, the existing bulges will change the propagating path of the streamer. The surface dielectric barrier discharge, which has been being investigated for a long time [7], such as the higher permittivity resulting in more intense gas discharge on the surface and higher surface charge density [8], the electron density distribution of SDBDs with positive and negative polarity differs from the each other near the powered electrode [9]. Researches referenced in 6-8 are all based on the condition that the dielectric barrier surface is flat. The influence mechanism of bulges on the SDBD is still not clear, which is important in the application of insulating material.

Coincidentally, this indicates that SDBD in the bulges may contribute to the surface charge accumulation. Therefore, the transportation process of charged species like electrons and ions would draw attention due to the bulges. The delivery and distribution characteristics of electrons and ions can bring new sight into the SDBD around the bulges on the dielectric barrier surface.

In this work, a two-dimensional self-consist fluid model is built to study SDBD with different bulges on the dielectric barrier. The spatio-temporal electron density distributions, electric field, and surface charge accumulations are studied with bulges' conditions of different depths and quantities. The length and path of streamer propagation are investigated, in order to find out how the bulges will change the propagating characteristics.

2. COMPUTATIONAL MODELL

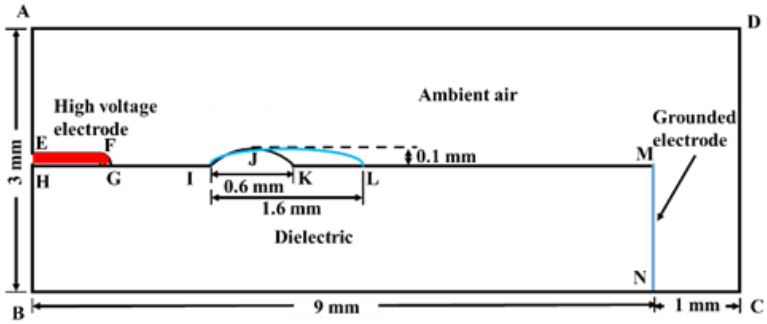

Fig. 1 Schematic of the geometry of the surface dielectric barrier discharge with bulges in the width of 0.8 mm and 1.6 mm respectively

As is depicted in Fig. 1, the simulation domain is 10 mm (length) ×3 mm (height). The grounded electrode is placed right side of the dielectric barrier, and the red electrode which is applied with high voltage is on the upper left surface of the dielectric. The height and the width of the red electrode are 0.2 mm, and 1 mm, respectively. The width of bulges on the surface selected is 0.6 mm and 1.6 mm on the dielectric barrier. The applied voltage is shown in Fig. 2. The time of rising edge and falling edge of the pulsed negative voltage is 5 ns, and the plateau value is −10 kV, with the total simulation time of 40 ns. The governing equations including continuity equations are given as follows:

$$\frac{\partial n_j}{\partial t} + \nabla \cdot \boldsymbol{j}_j = S_j \tag{1}$$

$$\boldsymbol{j}_{e,-} = -\mu_{e,-}\boldsymbol{E}n_{e,-} - D_{e,-}\nabla n_{e,-} \tag{2}$$

$$\boldsymbol{j}_{+} = \mu_{+}\boldsymbol{E}n_{+} - D_{+}\nabla n_{+} \tag{3}$$

$$\boldsymbol{j}_{m} = -D_{m}\nabla n_{m} \tag{4}$$

where n_j is the number density of the species j (j = e, –, +), $\boldsymbol{j}_j$ is the flux of species j (j = e, –, +). S_j is the source term of species j, obtaining from the chemical reactions. $\boldsymbol{E}$ is electric field strength, μ_j (j = e, –, +) is the charged particle mobility, D is the diffusion coefficient. The gas used in the simulation is simplified as the combination of 80% N_2 and 20% O_2, with the standard atmospheric pressure of 1×10^5 Pa. Besides, the model is a 2D finite element method simulation solving transport equations for all charged and neutral species and Poisson's equation. In order to get the more accurate solution from the complex geometry model, Finite Element Method (FEM) is applied to solve the problems. FEM has higher accuracy for solving complex structures. A commercial software COMSOL is applied to solve the problem, considering that it can integrate multiple physical fields, which is suitable for surface dielectric barrier discharge.

The electric field is calculated by the Poisson equation:

$$\nabla \cdot (\varepsilon_r \nabla \varphi) = -\rho/\varepsilon_0 \tag{5}$$

where φ is the electric potential and ρ is the space charge density, ε_0 is the vacuum permittivity. ε_r is the relative permittivity of dielectric barrier. Surface charge are calculated as follows:

$$\frac{\partial \sigma_s}{\partial t} = -e\left[\left(\sum \boldsymbol{j}_{+} - \sum \boldsymbol{j}_{-} - \boldsymbol{j}_e\right)\cdot \boldsymbol{n}\right] \tag{6}$$

$$\boldsymbol{j}_e \cdot \boldsymbol{n} = \left(-\mu_e \boldsymbol{E} n_e - \gamma \sum \boldsymbol{j}_{+}\right)\cdot \boldsymbol{n} \tag{7}$$

$$\boldsymbol{j}_{\pm} \cdot \boldsymbol{n} = \left(\mu_{\pm}\boldsymbol{E}\, n_{\pm} - D_{\pm}\nabla n_{\pm}\right)\cdot \boldsymbol{n} \tag{8}$$

where $\boldsymbol{n}$ is the unit vector perpendicular to the dielectric surface, σ_s is the surface charge density. γ is the secondary emission coefficient. $\boldsymbol{j}_j$ is the flux of species j (j = e, –, +), $\boldsymbol{E}$ is electric field strength, μ_j (j = e, –, +)

is the charged particle mobility, D is the diffusion coefficient. The secondary emission electron energy is set to 2.5 eV. In non-uniform distorted electric field, it is generally considered that the initial charged particle density obeys Gaussian distribution. The initial electron distribution is given by [10–12]:

$$n_e = N_{\max} \exp\left(-\frac{(x-x_1)^2 + (y-y_1)^2}{2\sigma^2} \right) \tag{9}$$

where $N_{\max} = 10^{16}\,\mathrm{m}^{-3}$, $\sigma = 62.5$ μm, representing the dispersion degree of the initial electron cloud and the needle pole. (x_1, y_1) is the spatial coordinates of needle electrode head.

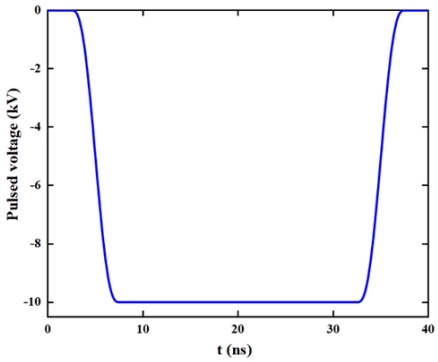

Fig. 2 – Pulsed negative voltage applied to the exposed electrode, the width of the pulse is 40 ns.

3. RESULTS AND DISCUSSION

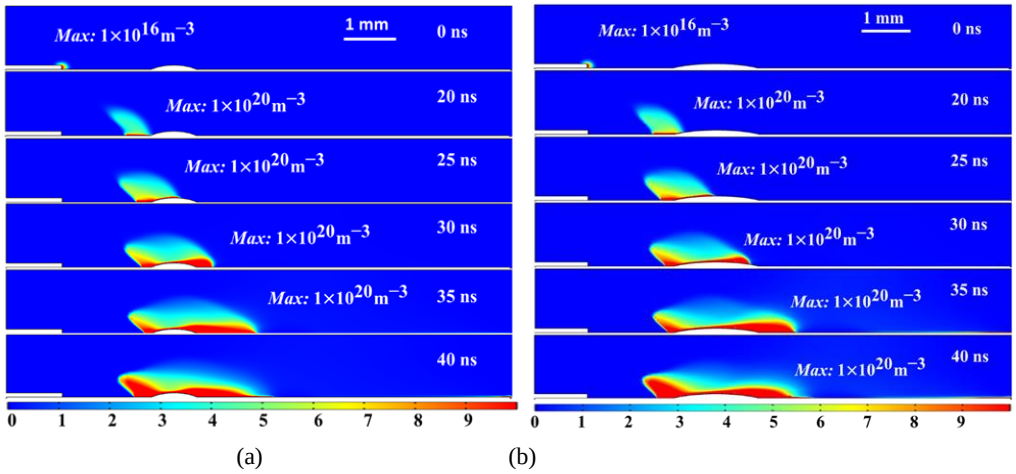

Fig. 3 – Spatial distribution of electron density at different times during a voltage pulse on bulge with 0.8 mm width (a) and 1.6 mm width (b).

The spatial electron density evolution on the bulges of 0.6 mm and 1 mm width on dielectric surface is shown in Fig. 3. As depicted in Fig. 3, within the first 20 ns, the negative discharge transfers from corona-like into streamer-like discharge, mainly due to the raise of the applied negative voltage at the initial stage. With the increase of the voltage value, the front of the streamer moves forward. When the streamer slides along the dielectric surface, it travels much faster when the pulsed voltage reaches –10kV, following a gas breakdown. The profiles in Fig. 3a shows the electric density distribution evolution on the bulges with 0.6 mm height. In Fig. 3b, it can be obtained that the propagation of the streamer is the same within 20 ns, before the streamer body reaching the left side of the bulge. When the head of the streamer arrives the left side of the bulges, after t = 25 ns, it moves with a further distance on the bulge with 1.6 mm width, which has a larger curvature. This indicates that with the existence of bulges with larger curvature, the streamer can propagate with a longer

distance. Besides, the streamer front at t = 35 ns in Fig. 3b gains a larger distribution area in height, the extend of the curvature of the bulges contributes to the diffusion process of the electrons, running into the air. At t = 40 ns, due to the fall of applied negative voltage value, the external electric field strength puts weak repulsion effect on the charged particles, so the reversal of the electron density distribution spatially appears in Fig. 3b. These results can be attributed to the electric field distribution. The electric field intensity plays a dominant role in the transporting process according to equation (2). The bulges on the dielectric barrier cause the distortion of the electric field over the bulges, and the distortion degree increases with the width of the bulge. As is indicated in Fig. 3b, more serious electric field distortion results in a relative considered ionization rate, producing more electron seeds in the front of the streamer, and bringing a faster propagating speed. With a slight rise in height of the dielectric barrier, the electric field line can be along the surface instead of spreading into the air. Finally, it results in the streamers propagating closer to the surface on the dielectric barrier. On the left half of the bulges, because the electric field is gradually concentrated along the bulge surface, the propagation path is much thinner, the electrons are cling to the bulge's surface. On the other half side of the bulge, the electron density distribution is more dispersed, motivated by the weaker electric field strength.

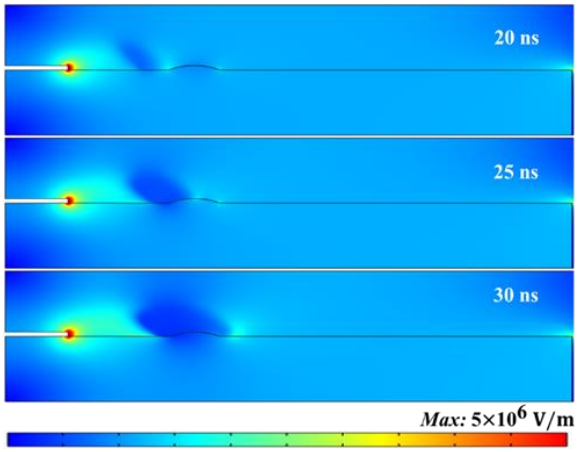

Fig. 4 – Electric filed distribution with bulge of 0.8 mm width on the surface at t = 20 ns, 25 ns and 30 ns.

As is depicted in Fig. 4, electric field distribution is concentrated on both edges of the bulges, which represents higher ionization rate locally. The electric field distribution is consisted of the contribution of the applied voltage and the part of locally charge density accumulation on the barrier surface. At t = 20 ns, when the front of the streamer starts to 'climb' on the surface of the bulge, the distorted electric field strength results in the accumulation of the electron density, as is shown in Fig. 3. These accumulated electrons will be the preparation of electrons reversal at the falling stage of the applied voltage . When the streamer strides over the bulge, at t = 30 ns, the concentrated electric filed in the figures indicates the coupling effect of the pre-ionization.

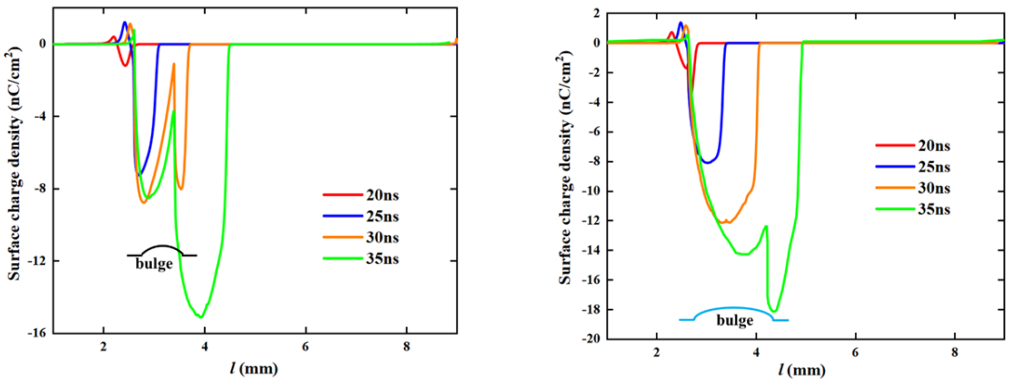

Fig. 5 – Surface charge density along the dielectric with bulge's width of 0.8 mm (a) and 1.6 mm (b).

As is shown in figures, surface charge density shows a much difference along the dielectric. Fig. 5 depicts two peak amplitudes of the surface charge density. The existence of the bulge with width of 0.8 mm retains a part of the surface charges, slowing down the propagating speed of the streamer on the bulged surface. At t = 30 ns, when the streamer travels at the right edge of the bulge, due to the different spread directions and speed, the right branch of the surface charge moves faster, as is indicated by t = 35 ns in Fig. 5a. Compared with Fig. 5a, Fig. 5b shows the similar trend of the surface charge density distribution. At the right edge of the bulge, there will be two branches of the surface charge density accumulation. The difference is that bulge with larger curvature results in higher accumulation of the surface charge on the bulges. These results from Fig. 5a and Fig. 5b can be attributed to the ionization rate difference and chemical reactions. As mentioned above, bulges with larger curvature cause higher distortion of the electric field distribution, more electrons are produced from the pre-ionization. Because some heavy species like N_2^+ has a slower moving speed than the electrons', according to the chemical reactions, the consumption collisions rate of electrons is lower. Besides, the distribution of the N_2^+ will significantly influence the momentum exchange process between the charged particles and neutral gas molecule in air.

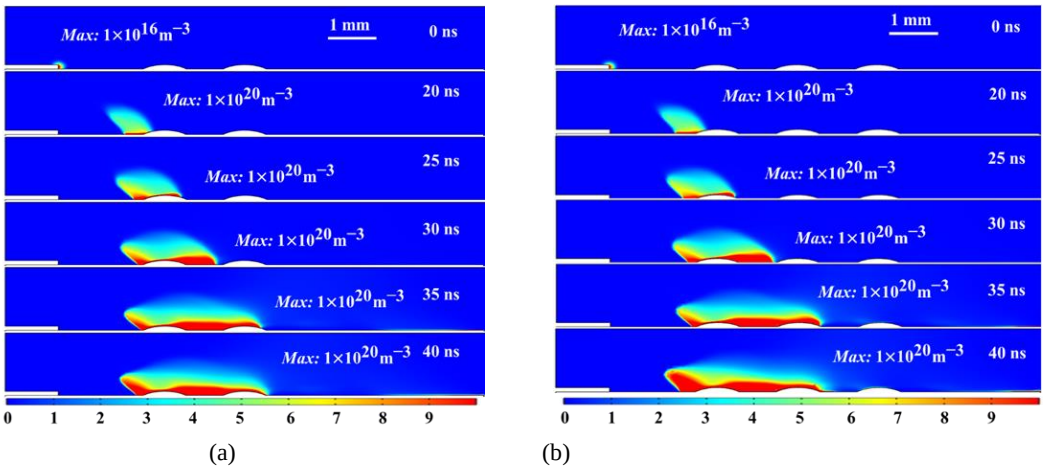

Fig. 6 – Spatial distribution of electron density at different times during a voltage pulse with two bulges (a), three bulges (b) of 0.8 mm in width and 0.1 mm in height.

Finally, in order to investigate the influence of multiple bulges on the surface dielectric barrier discharge, three bulges with height of 0.1 mm are applied. As is shown in Fig. 6a and Fig. 6b, electron density distribution before the falling edge of the applied voltage are similar with that in Fig. 3. At t = 40 ns, it is obvious that the reversal phenomenon of the electron density with three bulges is more serious, and between second and third bulges, pre-ionization appears, generating electrons distributed on the upper left side of the third bulge. Besides, the streamer front can slide with a longer distance adhesion to the surface of the dielectric barrier due to the pre-ionization. These results indicate that with the existence of the third bulge with 0.1 mm height, global electric field distribution will not be distorted intensely, but between the second and the third bulges, pre-ionization appears, which can not be observed between the first and the second ones.

In conclusion, with the same bulge's height (0.1 mm) selected, electric field distortion, surface charge accumulation and momentum exchange is more serious with the increase of the width of the bulge. When the quantity of bulges with smaller curvature is increased, the streamer can gain a longer propagation distance, changing the form that how the layer is charged in the surface. However, when the bulges with larger curvature appear on the dielectric barrier, the propagation is obstructed.

4. CONCLUSIONS

The following conclusions can be drawn from this study:

(1) With the increase of the bulge's width, the propagation distance of the streamer is extended, which means larger width will promote the distortion of the electric field, rising the ionization rate. This is helpful on the surface modification applications. Once the arrangement of the bulges on the barrier can be controlled, the efficiency of plasma assisted treatment can be improved.

(2) It can be obtained that surface charge accumulation changes with the bulge's width, no matter from the form or the number density. Changed surface charge distribution will play a dominant role in the streamer propagation, together with the distorted electric field. It changes even the number of density branches, accumulating directions, making it a more complex structure of surface charge during the streamer propagation.

(3) Finally, the quantity of the bulges make the streamer show different propagation path. With the increase of bulge quantities, the propagation of the streamer is hindered, but the ionization rate is improved between the subsequent bulges. Higher ionization rate can improve the efficiency in some medical use such as plasma disinfection. The reversal phenomenon at the tail of the streamer is more obvious, mainly due to the obstruction effect of the subsequent bulges.

REFERENCES

1. A. BOGAERTS, X. TU, J. C. WHITEHEAD, G. CENTI, L. LEFFERTS, O. GUAITELLA, J. F. AZZOLINA, H. H. KIM, A. B. MURPHY, W. F. SCHNEIDER, T. NOZAKI, J. C. HICKS, A. ROUSSEAU, F. THEVENET, A. KHACEF, M. CARREON, *The 2020 plasma catalysis roadmap*, Journal of Physics D: Applied Physics, **53**, *44*, p. 443001, 2020.
2. H.H. KIM, Y. TERAMOTO, A. OGATA, H. TAKAGI, T. NANBA, *Plasma catalysis for environmental treatment and energy applications*, Plasma Chemistry and Plasma Processing, **36**, *1*, pp. 45–72, 2016.
3. C.J. SHUAI, G.F. LIU, Y.W. YANG, W.J. YANG, C.X. HE, G.Y. WANG, Z. LIU, F.W. QI, S.P. PENG, *Functional BaTiO3 enhances piezoelectric effect towards cell response of bone scaffold*, Colloids & Surfaces B: Biointerfaces, **185**, p. 110587, 2020.
4. A. LIPOVKA, R. RODRIGUEZ, E. BOLBASOV, P. MARYIN, S. TVERDOKHLEBOV, E. SHEREMET, *Time-stable watting effect of plasma-treated biodegradable scaffolds functionalized with graphene oxide*, Surface & Coatings Technology, **388**, p. 125560, 2020.
5. A. ELTOM, G.Y. ZHONG, A. MUHAMMAD, *Scaffold techniques and designs in tissue engineering functions and purposes: a review*, Advances in Materials Science and Engineering, **2019**, p. 3429527, 2019.
6. M.G. SEO, M.J. TAHK, *Observability analysis and enhancement of radome aberration estimation with line-of-sight angle-only measurement*, IEEE Transactions on Aerospace and Electronic Systems, **51**, *4*, pp. 3321–3331, 2015.
7. V.R. SOLOVIEV, V.M. KRIVTSOV, *Numerical modelling of nanosecond surface dielectric barrier discharge evolution in atmospheric air*, Plasma Sources Science and Technology, **27**, *11*, p. 114001, 2018.
8. R. TSCHIERSCH, S. NEMSCHOKMICHAL, M. BOGACZYK, J. MEICHSNER, *Surface charge measurements on different dielectrics in diffuse and filamentary barrier discharges*, Journal of Physics D: Applied Physics, **50**, *10*, p. 105207, 2017.
9. V.R. SOLOVIEV, V.M. KRIVTSOV, S.A. SHCHERBANEV, S.M. STARIKOVSKAIA, *Evolution of nanosecond surface dielectric barrier discharge for negative polarity of a voltage pulse*, Plasma Sources Science and Technology, **26**, *1*, p. 014001, 2018.
10. R. MORROW, J. LOWKE, *Streamer propagation in air*, Journal of Physics D: Applied Physics, **30**, *4*, pp. 614–627, 1997.
11. W.S. KANG, J. PARK, Y. KIM, S. HONG, *Numerical study on influences of barrier arrangements on dielectric barrier discharge characteristics*, IEEE Transactions on Plasma Science, **31**, *4*, pp. 504–510, 2003.
12. T.N. TRAN, I.O. GOLOSNOY, P.L. LEWIN, G.E. GEORGHIOU, *Numerical modelling of negative discharges in air with experimental validation*, Journal of Physics D: Applied Physics, **44**, *1*, p. 015203, 2011.

Received December 27, 2023